CHALMERS
UNIVERSITY OF TECHNOLOGY

Investigation of Noise Properties in the InP HEMT for LNAs in Qubit Amplification: Effects From Channel Indium Content

Citation for the original published paper (version of record):
Li, J., Bergsten, J., Pourkabirian, A. et al (2024). Investigation of Noise Properties in the InP HEMT for LNAs in Qubit Amplification: Effects From
Channel Indium Content. IEEE Journal of the Electron Devices Society, 12: 243-248.
http://dx.doi.org/10.1109/JEDS.2024.3371905

Investigation of noise properties in the InP HEMT for LNAs in qubit amplification: Effects from channel indium content

Junjie Li, *Graduate Student Member, IEEE,* Johan Bergsten, Arsalan Pourkabirian, *Member, IEEE,* Jan Grahn, *Senior Member, IEEE*

***Abstract*—The InP high-electron-mobility transistor (HEMT) is employed in cryogenic low-noise amplifiers (LNAs) for the readout of faint microwave signals in quantum computing. The performance of such LNAs is ultimately limited by the properties of the active $\mathrm{In_xGa_{1-x}As}$ channel in the InP HEMT. In this study, we have investigated the noise performance of 100-nm gate-length InP HEMTs used in cryogenic LNAs for amplification of qubits. The channel indium content in the InP HEMTs was 53, 60 and 70%. Hall measurements of the epitaxial materials and dc characterization of the InP HEMTs confirmed the superior transport properties of the channel structures. An indirect method involving an LNA and small-signal noise modeling was used for extracting the channel noise with high accuracy. Under noise-optimized bias, we observed that the 60% indium channel InP HEMT exhibited the lowest drain noise temperature. The difference in LNA noise temperature among InP HEMTs became more pronounced with decreasing drain voltage and current. An average noise temperature and average gain of 3.3 K and 21 dB, respectively, for a 4-8 GHz three-stage hybrid cryogenic LNA using 60% indium channel InP HEMTs was measured at a dc power consumption of 108 μW. To the best of the authors' knowledge, this is a new state-of-the-art for a C-band LNA operating below 1 mW. The higher drain noise temperature observed for 53 and 70% indium channels InP HEMTs can be attributed to a combination of thermal noise in the channel and real-space transfer of electrons from the channel to the barrier. This report gives experimental evidence of an optimum channel indium content in the InP HEMT used in LNAs for qubit amplification.**

***Index Terms*—Drain noise temperature, InP high-electron-mobility transistor (HEMT), indium channel, low-noise amplifier (LNA), qubit amplification.**

I. Introduction

The cryogenic InP high-electron-mobility transistor (HEMT) low-noise amplifiers (LNAs) are today used in amplification of qubits at 4 K in the 4-8 GHz band [1], [2]. Since the power of the qubit is extremely small, the signal-to-noise ratio of the LNA must be highest possible. In the InP HEMT, the $\mathrm{In_xGa_{1-x}As}$ channel plays a decisive role in the final noise properties of the HEMT LNAs [3], [4]. The well-known Fukui equation stipulates that the higher transconductance g_m for the HEMT, the lower the noise figure [5]. Since g_m is directly related to the velocity of the charge carriers [6], the obvious material parameter to increase for lower noise is the mobility of the channel electrons in the HEMT. The electron mobility in the two-dimensional electron gas (2DEG) of $\mathrm{In_xGa_{1-x}As}$ channel is well-known to increase with its indium content [7]. However, several recent reports have shown that increasing electron mobility by higher channel indium content in the InP HEMT does not necessarily guarantee noise reduction. For example, [8] showed that an InP HEMT with a higher indium channel (5 nm InAs inset) exhibited higher noise than 2 nm InAs inset channel at room temperature. Additionally, [3] reported that an LNA with x = 80% channel InP HEMT experienced nearly twice the amount of noise compared to x = 65% at 4 K, despite similar noise level for the LNAs at room temperature [3]. A study by Heinz *et al.* [4] indicated that a single $\mathrm{In_xGa_{1-x}As}$ channel with x = 80% in cryogenic metamorphic HEMT LNAs achieved the lowest noise among studied channel structures within the 8-18 GHz frequency range. The same study revealed that a composite $\mathrm{In_{0.8}Ga_{0.2}As/In_{0.53}Ga_{0.47}As}$ channel displayed a larger noise reduction upon cooling than a $\mathrm{In_{0.65}Ga_{0.35}As/In_{0.53}Ga_{0.47}As}$ channel, resulting in nearly identical noise temperatures for both structures within the same frequency range at 10 K. To conclude, recent reports of InP HEMTs with various channel indium content suggest a non-trivial dependence with respect to final noise properties of the HEMT and LNA. This calls for careful calibration of the parameter x, *i.e.* the channel indium content, for the lowest noise in the InP HEMT LNA.

In this paper, we report the first investigation of noise properties at 5 K for the 100-nm gate-length InP HEMTs where channel indium content was varied with x = 53, 60 and 70%. It was found that x = 60% was the optimum channel indium content. A physical explanation for the optimum is discussed involving thermal noise and real-space transfer of electrons in the 2DEG of the InP HEMT. Since the transistor noise was extracted in the 4-8 GHz range at 5 K, the results here are of direct relevance for the choice of the InP HEMT in cryogenic LNAs used for the processing of qubits.

Corresponding author: Junjie Li. Email: junjiel@chalmers.se

Junjie Li and Jan Grahn are with the Department of Microtechnology and Nanoscience, Chalmers University of Technology, SE-41296 Gothenburg, Sweden

Johan Bergsten and Arsalan Pourkabirian are with Low Noise Factory AB, SE-41263 Gothenburg, Sweden

Manuscript received October xx, 2023.

II. HEMT channel design

Three different indium levels x = 53, 60 and 70% in the active $\mathrm{In_xGa_{1-x}As}$ channel of the InP HEMT were investigated in this study [9]. To compensate for the different amount of

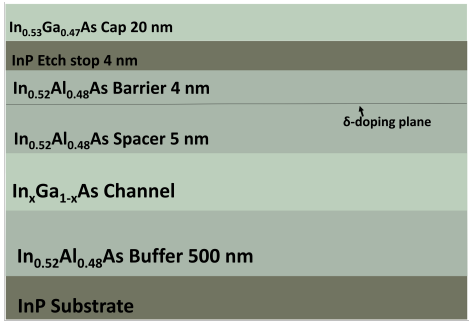

Fig. 1. Schematic of InP HEMT epitaxial layers with channel indium content x = 53%, 60% and 70%.

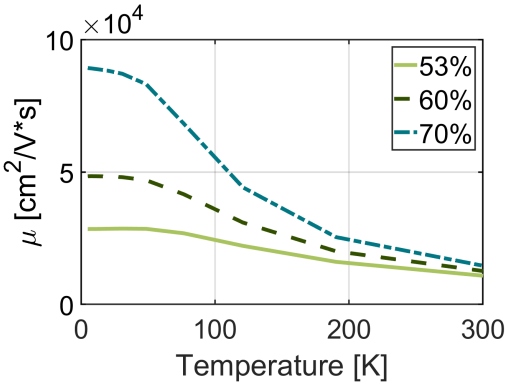

Fig. 2. The μ versus temperature from 5 K to 300 K for 53% (light green solid), 60% (dark green dashed) and 70% (blue dash-dot) indium channel without cap layers.

strain in the channel, the thickness was 15, 20 and 10 nm for x = 53, 60 and 70%, respectively. While 53% corresponded to a lattice-matched HEMT, 60% and 70% meant strained channels still below their critical thickness. Simulations showed that the 2DEG was confined to the InAlAs-InGaAs interface [10]. Since the transistor was operated at a low drain current for low noise operation, the difference in channel thickness should not affect the device noise results for the InP HEMTs investigated here. Apart from the channel, the epitaxial structures for the three InP HEMTs were identical. See Fig. 1 for details of the epitaxial layers used for InP HEMT fabrication [11].

The electron sheet carrier concentration n_{sh} for all channels was 2.5×10^{12} cm^{-2} with less than 10% variation, as determined by Hall measurements. While the n_{sh} remained constant with temperature, the Hall electron mobility μ in the channel increased with reduced temperature and higher channel indium content, as shown in Fig. 2. The increase in μ with indium concentration was higher at lower temperatures. Below 50 K, the increase in mobility flattened out. Around 5 K, the μ ended up at 28,000, 48,000 and 89,000 cm^2/Vs for 53, 60 and 70% indium channel, respectively. Such mobility numbers confirm the high quality of the active channel materials used for the InP HEMTs [3], [12].

III. Results

InP HEMTs with a gate length of 100 nm and a gate width of 4×50 μm were fabricated using the method detailed in Refs.

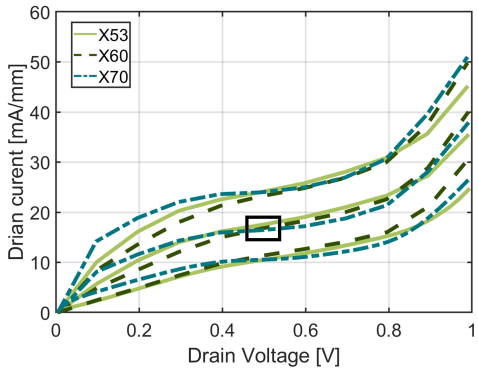

Fig. 3. The I_d-V_{ds} characteristics of the 100 nm gate length InP HEMT using 4 × 50 μm gate-width layout with channel indium content of 53% (light green solid), 60% (dark green dashed) and 70% (blue dash-dot) at 5 K. The open rectangle around V_{ds}=0.5 V highlights the low-noise bias region used for the HEMTs. For X53, V_{gs}= 0.20, 0.21 and 0.22 V. For X60 and X70, V_{gs}=0.24, 0.25 and 0.26 V.

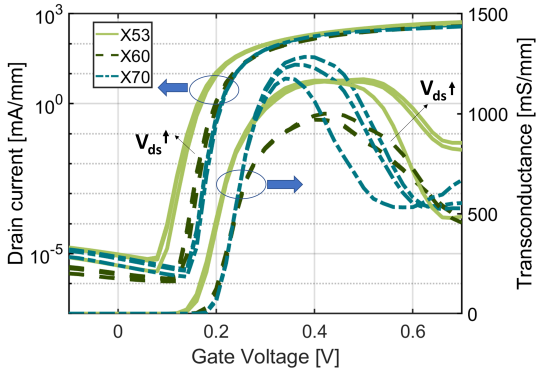

Fig. 4. The I_d-V_{gs} and transconductance of the 100 nm gate length InP HEMT using 4 × 50 μm gate-width layout with channel indium of 53% (light green solid), 60% (dark green dashed) and 70% (blue dash-dot) at 5 K. V_{ds}=0.4, 0.5 and 0.55 V.

[13] and [14]. Fig. 3 displays the output dc characteristics at 5 K for the InP HEMTs with 53% (X53), 60% (X60) and 70% (X70) channel indium content. The lowest-noise bias region for the InP HEMTs, illustrated with an open rectangle in Fig. 3, corresponded to a drain current $I_d \sim 15$ mA/mm and a drain voltage $V_{ds} \sim 0.5$ V [14]. To achieve the same I_d for different devices, the gate voltage V_{gs} must be varied. Fig. 4 illustrates the I_d and g_m as a function of V_{gs} at 5 K. It is observed that the threshold voltage V_{th} is 0.10 V, 0.16 V and 0.14 V for X53, X60 and X70, respectively. It is worth noting that the g_m curve for X70 is the highest and narrowest among the three InP HEMTs. This indicates that X70 has the highest gain and cutoff frequency [6], [8]. Compared with X53 and X60, the X70 reveals the steepest increase in g_m versus V_{gs} which results in the smallest value of $\sqrt{I_{ds}}/g_m$ at the optimum low-noise bias (with 0.20, 0.21 and 0.16 $\sqrt{V \cdot mm/S}$ for X53, X60 and X70, respectively). According to [15], this signifies that X70 will have the lowest noise among the three devices in Fig. 4. As will be shown below, this conclusion is not correct.

A valid noise comparison between InP HEMTs at cryogenic temperature depends on high accuracy in the noise measure-

ment. We selected an indirect method using a hybrid 4-8 GHz three-stage LNA mounted with discrete InP HEMTs [16], [17]. This procedure yields more than 10 times higher accuracy in HEMT noise estimation than an on-wafer measurement involving device probing in a cryostat [18], [19]. The noise of the InP HEMT was measured in the LNA by the Y-factor method using a cold attenuator at 5 K [16], [17]. Provided the LNA gain was higher than 40 dB, the absolute measurement uncertainty for the LNA average noise temperature $T_{N,avg}$ was determined to be less than 0.3 K [18]. The measurement repeatability was estimated to be better than 0.05 K.

Fig. 5 displays the gain and noise temperature T_N of the three LNAs at 5 K equipped with InP HEMTs X53, X60 and X70. All LNAs were noise-optimized at an LNA drain voltage V_{DS} = 0.7 V and drain current I_D = 11 mA. The LNA with X70 exhibited the highest gain of 45 dB whereas the LNAs with X53 and X60 showed 41 dB gain. Such high values meant high precision in the noise measurements. The $T_{N,avg}$ measured 1.4 K (noise figure (NF) = 0.021 dB) for the LNA with X53 and 1.2 K (NF = 0.018 dB) for both X60 and X70 LNAs. Despite its higher gain, the LNA with X70 did not end up in reduced $T_{N,avg}$ compared to the LNA with X60. This indicates that the X70 InP HEMTs have higher noise power than X60.

The noise measurement procedure described in [16] made it possible to extract the noise temperature of the first-stage InP HEMT in the LNA. In Fig. 6, it is observed that the first-stage noise temperature of X70 is slightly higher than X60 (0.02 K). Such small differences in noise between the InP HEMTs can be studied by plotting the $T_{N,avg}$ and average gain G_{avg} versus the LNA DC power $P_{DC} = V_{DS} \times I_D$; See Fig. 7. To ensure $T_{N,avg}$ remained at its minimum number for all P_{DC}, the V_{gs} bias was kept nearly constant with values of 0.2 V, 0.25 V, and 0.25 V for X53, X60, and X70, respectively. In Fig. 7a, the $T_{N,avg}$ of X60 is lower than X70 for reduced P_{DC} values thus confirming the observation in noise temperature for the first stage in Fig. 6. Furthermore, this coincides with a reduced gain difference between X60 and X70 at P_{DC} lower than 1 mW (Fig. 7b). The LNA with X53 showed lower gain and higher noise compared to the LNAs with X60 and X70 in Fig. 7. In comparison to the 4-8 GHz LNA result at 300 μW reported in [20], the best $T_{N,avg}$ in Fig. 7a was 0.9 K lower with the same G_{avg} = 23 dB. The LNA equipped with X60 demonstrated a $T_{N,avg}$ = 3.3 K (NF = 0.049 dB) and G_{avg} = 21 dB at a P_{DC} of 108 μW. To our knowledge, this is a new state-of-the-art noise and gain for a C-band LNA operating below 1 mW.

The drain noise temperature T_d of the InP HEMT is an empirical model parameter derived from the LNA noise measurement in Fig. 5 [21], [22]. The model requires extraction of the intrinsic parameters in the InP HEMT. This is achieved by a small-signal model (SSM) approach based on S-parameter data for the InP HEMT recorded on-wafer in a probe station [21], [23]. The SSM data was taken at the same temperature (5 K) as used for the LNA measurement in Fig. 5. In the SSM, the gate current I_g was treated as a frequency-independent shot noise source. The gate noise temperature T_g was set to 10 K, considering the self-heating effect in the HEMT [24]. The T_d

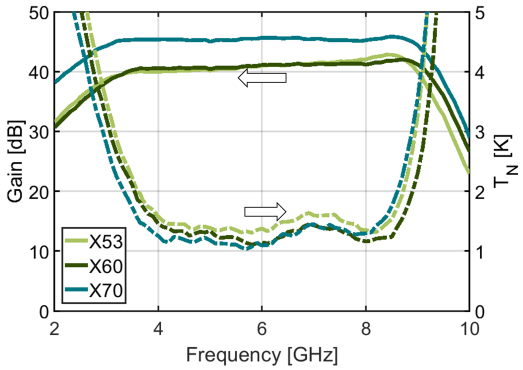

Fig. 5. The measured gain (solid) and noise temperature (dashed) of three-stage 4-8 GHz hybrid LNAs integrated with the 100 nm InP HEMT with channel indium content of 53% (light green), 60% (dark green) and 70% (blue) at an ambient temperature of 5 K. The optimum noise bias for all LNAs was V_{DS} = 0.7 V and I_D= 11 mA.

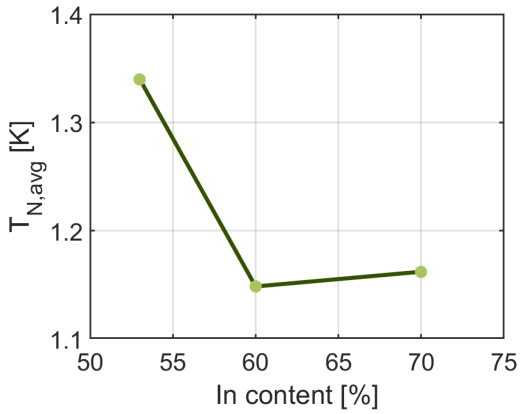

Fig. 6. The first-stage noise temperature extracted from the three-stage InP HEMT LNAs as a function of channel indium content at an ambient temperature of 5 K.

can be determined by fitting the measured and simulated T_N. Fig. 8 depicts the extracted T_d at the lowest noise bias for the InP HEMT together with the μ versus channel indium content at 5 K. Even though the extraction of T_d normally is associated with an inaccuracy of up to $\pm$ 100 K, Fig. 8 shows a minimum in T_d versus channel indium content. In contrast, μ showed an almost linear increase. Compared to X60, the X70 was 20% higher in T_d at the optimum noise bias. We conclude that for lowest T_d, there seems to be an optimum channel indium content not corresponding to its highest electron mobility.

With knowledge of the three-stage amplifier circuit, the V_{ds} and I_d of the InP HEMT can be calculated from the V_{DS} and I_D (determining P_{DC}) of the LNA. In Fig. 9, T_d is plotted versus V_{ds} for InP HEMTs X53, X60 and X70. As expected, an increase in T_d with V_{ds} is observed for all devices [25]. The X60 shows a lower T_d than X53 and X70 over the whole bias range in V_{ds}. Additionally, the drain noise of the 70% indium channel is similar to that of the 53% channel at high V_{ds}. At lowest V_{ds}, the X70 becomes even higher in T_d than the X53.

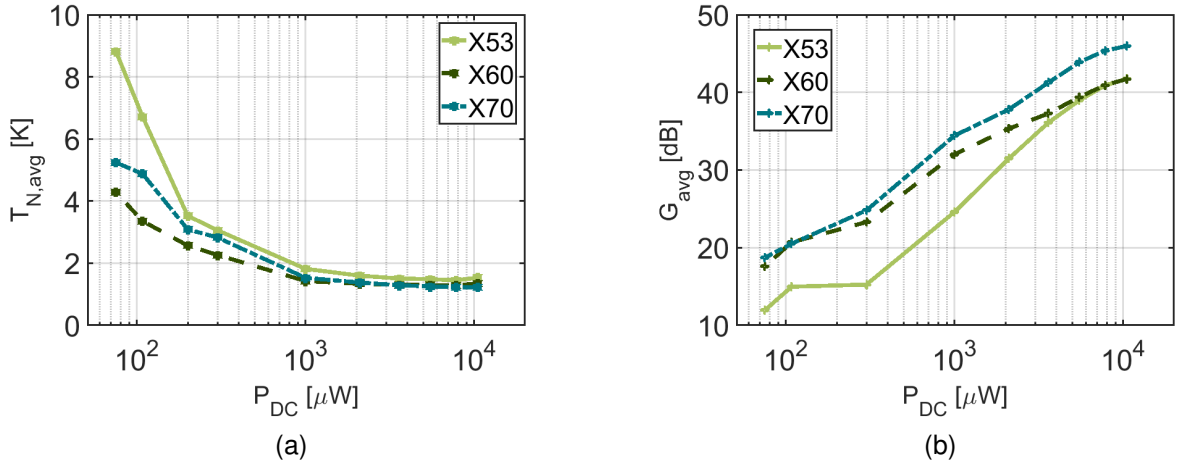

Fig. 7. (a) The average noise temperature and (b) the average gain as a function of dc power dissipation P_{DC} for InP HEMT LNAs with 53% (light green solid), 60% (dark green dashed) and 70% (blue dash-dot) indium channel at 5 K.

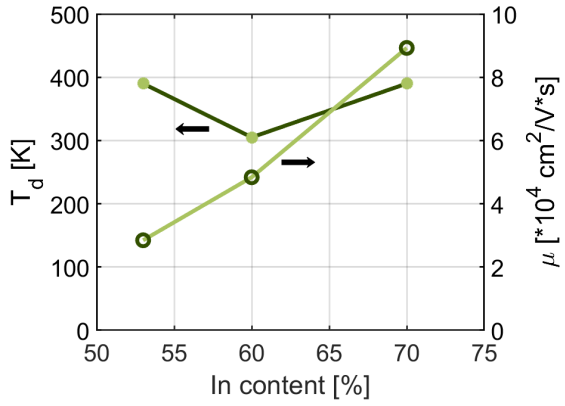

Fig. 8. The drain noise temperature T_d (dark green line to the left axis) extracted at optimum noise bias of V_{DS} = 0.7 V and I_D = 11 mA and Hall electron mobility μ (light green line to the right axis) of the InP HEMT as a function of channel indium content at 5 K.

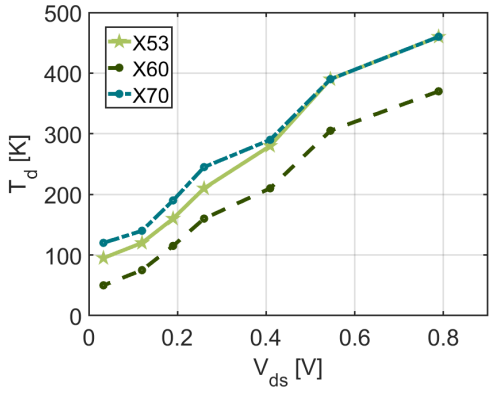

Fig. 9. T_d as a function of V_{ds} for InP HEMT with 53% (light green solid), 60% (dark green dashed) and 70% (blue dash-dot) indium channel at 5 K.

IV. Discussion

To analyze the various noise contributions in the LNA, we used a circuit simulator based upon an established small-signal noise model for the HEMT [22]. The simulations were carried out for InP HEMTs with different channel indium content. To evaluate the individual contribution from each noise source, all noise sources but for the studied one were set to zero. Fig. 10 illustrates the relative contribution for each noise source at optimum noise bias in the HEMT LNA at 6 GHz. All simulations were performed at 5 K. The bar chart in Fig. 10 reveals that several circuit elements including matching network, gate resistance R_g and intrinsic gate-source resistance R_i, marginally contribute to the total cryogenic LNA noise. As expected, the high indium content X70 generates a relatively high shot noise contribution in the LNA due to a higher I_g [26]. However, I_g contribution to the total noise is not dominant. Conversely, the intrinsic channel output conductance g_{ds} stands out as the primary factor for the total LNA noise temperature which highlights the importance of channel noise in the InP HEMT. As a result, T_d, $i.e.$ the equivalent noise temperature for g_{ds} [22], is the most representative parameter for the noise level of the InP HEMT used in cryogenic LNAs at microwave frequencies.

The higher T_d for 70% indium channel HEMT than 60% seen in Fig. 8 cannot be ascribed to impact ionization. While richer indium channels normally experience stronger impact ionization, its occurrence is highly unlikely in the low-noise bias region [3], [27]. Moreover, impact ionization is typically accompanied by a significant increase in gate current [26]. In this study, the I_g remained below 0.1 μA at all biases. The extraction of T_d already accounted for the I_g by modeling it as shot noise; The 6% difference in shot noise between X70 and X60 does not explain the 20% difference observed in T_d.

The T_d is associated with the level of channel carrier fluctuations. The noise in the HEMT channel is normally attributed to thermal noise and excess noise [28]. It has been reported that the real-space transfer (RST) noise constitutes a dominant contribution to the excess noise for the cryogenic InP HEMT at high bias [11], [28], [29]. In contrast, the thermal noise is present across the entire electrical field range. The thermal noise in the channel is proportional to $k_B T g_{ds0}$ where

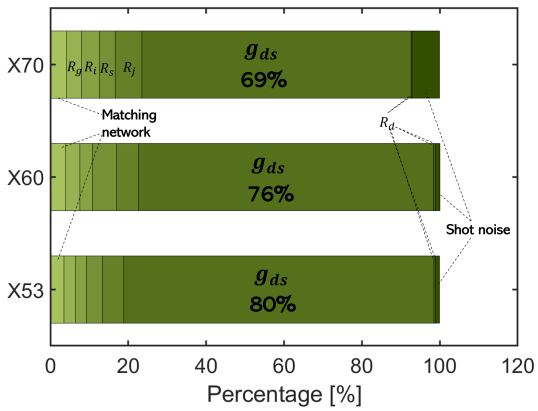

Fig. 10. Simulated contribution for each noise source at the optimum noise bias in the three-stage InP HEMT LNA at 6 GHz. The InP HEMTs were of 53%, 60% and 70% indium channel (X53, X60, and X70). All simulations carried out at 5 K.

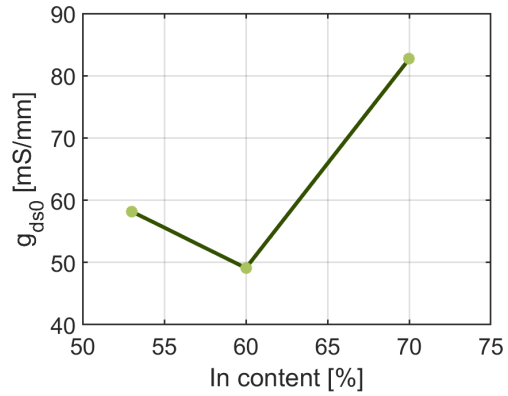

Fig. 11. The output conductance extrapolated at zero V_{ds} versus channel indium content at the V_{gs} used for noise extraction.

k_B is the Boltzmann constant, T is the lattice temperature and g_{ds0} is the output conductance at zero drain bias [30]. In Fig. 11, g_{ds0}, extrapolated from data in Fig. 3, is plotted for X53, X60 and X70 InP HEMTs. We note that g_{ds0} displays an agreement with the T_d behavior for different channel indium content at low V_{ds} in Fig. 9.

The RST noise in the InP HEMT depends on the conduction band offset ΔE_c between channel and barrier, and the overdrive voltage $V_{ov} = V_{gs} - V_{th}$ of the transistor [11], [29]. The ΔE_c experiences a rapid increase of 0.12 eV from X53 to X60 as illustrated in the right y-axis of Fig. 12. At the same time, V_{ov} exhibits a minimum for X60, see left y-axis in Fig. 12. The ΔE_c and V_{ov} predicts a higher RST noise contribution for X53 than for X60 and X70 at high V_{ds}; See the steeper increase with V_{ds} for X53 in Fig. 9. At low V_{ds}, the thermal noise starts to dominate and the T_d of X53 becomes even lower than for X70. At all biases, X60 has the lowest total channel noise.

V. Conclusion

We have characterized the noise for cryogenic InP HEMTs where the channel noise dominates the total noise behavior.

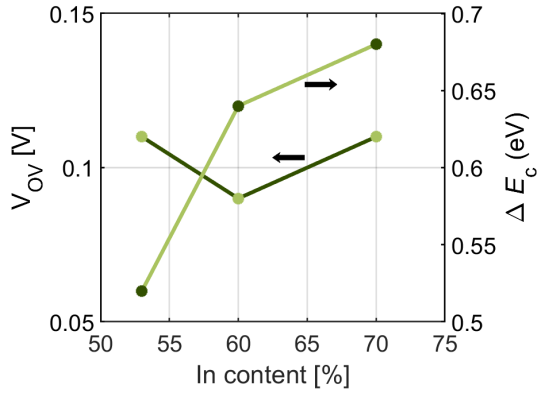

Fig. 12. The overdrive voltage at the optimum noise gate bias and the conduction band offset as a function of the channel indium content.

InP HEMTs with channel indium content from 53 to 70% were investigated. The corresponding 4-8 GHz cryogenic InP HEMT LNAs exhibited similar noise at high P_{DC}. For reduced P_{DC}, the LNA with X60 demonstrated lower noise than X53 and X70. The higher T_d of X53 and X70 was explained by a noise model for the channel in the HEMT taking the thermal and RST noise contributions into account. The results showed that the 60% indium channel is the best choice for the InP HEMT in low-noise and low-power cryogenic LNAs at microwave frequencies. An average noise temperature of 3.3 K was measured for a 4-8 GHz cryogenic LNA at 108 μW dc power. The results in this study are of significance for the selection of InP HEMTs in LNAs used in qubit amplification.

Acknowledgments

The authors express their gratitude to Alexei Kalaboukhov at Chalmers University of Technology for conducting the Hall measurements. They also extend their appreciation to Jörgen Stenarson and Estefany Santana at Low Noise Factory AB for valuable assistance with mapping and noise measurement. Additionally, the authors are thankful to Bekari Gabritchidze, Anthony J. Ardizzi, Jiayin Zhang, and Austin J. Minnich at Caltech, as well as Dae-Hyun Kim from Kyungpook National University, for fruitful discussions. This work was supported in part by the Swedish Research Council. Device fabrication was performed at Myfab Chalmers. This research has been carried out in Gigahertz-ChaseOn Bridge Centre in the CRYTER project financed by Low Noise Factory, Virginia Diodes, AAC Omnisys, Chalmers, and Vinnova.

References

[1] J. C. Bardin, D. H. Slichter, D. J. Reilly, "Microwaves in Quantum Computing", *IEEE Journal of Microwaves*, vol.1, no.1, pp. 403-427, 2021. doi:10.1109/JMW.2020.3034071.

[2] J. M. Hornibrook, J. I. Colless, I. D. Conway Lamb, S. J. Pauka, H. Lu, A. C. Gossard, J. D. Watson, G. C. Gardner, S. Fallahi, M. J. Manfra, D. J. Reilly, "Cryogenic control architecture for large-scale quantum computing", *Phys. Rev. Appl.*, vol. 3, no. 2, 2015, doi:10.1103/PhysRevApplied.3.024010.

[3] E. Cha, N. Wadefalk, G. Moschetti, A. Pourkabirian, J. Stenarson, J. Li, D-H Kim, J. Grahn, "Optimization of channel structures in InP HEMT technology for cryogenic low-noise and low-power operation", *IEEE Transactions on Electron Devices*, vol. 70, no. 5, pp. 2431-2436, 2023, doi:0.1109/TED.2023.3255160.

[4] F. Heinz, F. Thome, A. Leuther, O. Ambacher, "A 50-nm gate-length metamorphic HEMT technology optimized for cryogenic ultra-low-noise operation", *IEEE Transactions on Microwave Theory and Techniques*, vol. 69, no. 8, pp. 3896-3907, 2021, doi:10.1109/TMTT.2021.3081710.

[5] H. Fukui, "Optimal noise figure of microwave GaAs MESFET's", *IEEE Transactions on Electron Devices*, vol. 26, no. 7, pp. 1032-1037, 1979, doi:10.1109/T-ED.1979.19541.

[6] S. M. Sze, K. K. Ng "Physics of semiconductor devices", *John Wiley & Sons.*, 2006.

[7] F. Schwierz, J. J. Liou, "Modern microwave transistors: theory, design, and performance", *Wiley*, 2002.

[8] D. C. Ruiz, T. Saranovac, D. Han, A. Hambitzer, A. M. Arabhavi, O.r Ostinelli, C. R. Bolognesi, "InAs channel inset effects on the DC, RF, and noise properties of InP pHEMTs", *IEEE Transactions on Electron Devices*, vol. 66, no. 11, pp. 4685-4691, 2019, doi:10.1109/TED.2019.2940638.

[9] J. Li, J. Bergsten, A. Pourkabirian, N. Wadefalk, J. Grahn, "Optimization of InGaAs channel for cryogenic InP HEMT low-noise amplifiers", *2023 Compound Semiconductor Week (CSW)*, 2023.

[10] Helena Rodilla, Joel Schleeh, Per-Ake Nilsson, Niklas Wadefalk, Javier Mateos, Jan Grahn, "Cryogenic performance of low-noise InP HEMTs: A Monte Carlo study", *IEEE Transactions on Electron Devices*, Vol. 60, no. 5, pp. 1625-1631, 2013. doi:10.1109/TED.2013.2253469.

[11] J. Li, A. Pourkabirian, J. Bergsten, N. Wadefalk, J. Grahn, "Influence of spacer thickness on the noise performance in InP HEMTs for cryogenic LNAs", *IEEE Electron Device Letters*, vol. 43, no. 7, pp. 1029-1032, 2022, doi:10.1109/LED.2022.3178613.

[12] Y-W Chen, W-C Hsu, R-T Hsu, Y-H Wu, Y-J Chen, "Characteristics of $In_{0.52}Al_{0.48}As/In_xGa_{1-x}As$ HEMT's with various $In_xGa_{1-x}As$ channels", *Solid-State Electronics*, Vol. 48, no. 1, pp. 119-124, 2004. doi:10.1016/S0038-1101(03)00287-9.

[13] E. Cha, N. Wadefalk, G. Moschetti, A. Pourkabirian, J. Stenarson, J. Grahn, *"InP HEMTs for sub-mW cryogenic low-noise amplifiers"*, *IEEE Electron Device Letters*, vol. 41, no. 7, pp. 1005-1008, 2020, doi:10.1109/LED.2020.3000071.

[14] J. Li, A. Pourkabirian, J. Bergsten, N. Wadefalk, J. Grahn, "On the relation between rf noise and subthreshold swing in InP HEMTs for cryogenic LNAs", *2022 Asia-Pacific Microwave Conference (APMC)*, 2022, doi:10.23919/APMC55665.2022.9999771.

[15] M. W. Pospieszalski, "Extremely low-noise amplification with cryogenic FETs and HFETs: 1970-2004", *IEEE Microwave Magazine*, vol. 6, no. 3, pp. 62-75, 2005, doi:10.1109/MMW.2005.1511915.

[16] N. Wadefalk, A. Mellberg, I. Angelov, M.E. Barsky, S. Bui, E. Choumas, R.W. Grundbacher, E.L. Kollberg, R. Lai, N. Rorsman, P. Starski, J. Stenarson, D.C. Streit, H. Zirath, "Cryogenic wide-band ultra-low-noise IF amplifiers operating at ultra-low DC power", *IEEE Transactions on Microwave Theory and Techniques*, vol. 51, no. 6, pp. 1705-1711, 2003, doi:10.1109/TMTT.2003.812570.

[17] J. L. Cano, N. Wadefalk, J. D. Gallego-Puyol, "Ultra-wideband chip attenuator for precise noise measurements at cryogenic temperatures", *IEEE Transactions on Microwave Theory and Techniques*, vol. 58, no. 9, pp. 2504-2510, 2010, doi:10.1109/TMTT.2010.2058276.

[18] J. Randa, E. Gerecht, Dazhen Gu, R.L. Billinger, "Precision measurement method for cryogenic amplifier noise temperatures below 5 K", *IEEE Transactions on Microwave Theory and Techniques*, vol. 54, no. 3, pp. 1180-1189, 2006, doi:10.1109/TMTT.2005.864107.

[19] J. Laskar, J.J. Bautista, M. Nishimoto, M. Hamai, R. Lai, "Development of accurate on-wafer, cryogenic characterization techniques", *IEEE Transactions on Microwave Theory and Techniques*, vol. 44, no. 7, pp. 1178-1183, 1996, doi:10.1109/22.508659.

[20] E. Cha, N. Wadefalk, G. Moschetti, A. Pourkabirian, J. Stenarson, J. Grahn, "A 300-μW cryogenic HEMT LNA for quantum computing", *2020 IEEE/MTT-S International Microwave Symposium (IMS)*, pp. 1299-1302, 2020, doi:10.1109/IMS30576.2020.9223865.

[21] M. W. Pospieszalski, "Modeling of noise parameters of MESFETs and MODFETs and their frequency and temperature dependence", *IEEE Transactions on Microwave Theory and Techniques*, vol. 37, no. 9, pp. 1340-1350, 1989, doi:10.1109/22.32217.

[22] J. Schleeh, N. Wadefalk, P. Å. Nilsson, J. P. Starski and J. Grahn, "Cryogenic Broadband Ultra-Low-Noise MMIC LNAs for Radio Astronomy Applications", *IEEE Transactions on Microwave Theory and Techniques*, vol. 61, no. 2, pp. 871-877, 2013, doi:10.1109/TMTT.2012.2235856.

[23] N. Rorsman, M. Garcia, C. Karlsson, H. Zirath, "Accurate small-signal modeling of HFET's for millimeter-wave applications", *IEEE Transactions on Microwave Theory and Techniques*, vol. 44, no. 3, pp. 432-437, 1996, doi:10.1109/22.486152.

[24] A. J. Ardizzi, A. Y. Choi, B. Gabritchidze, J. Kooi, K. A. Cleary, A. C. Readhead, A. J. Minnich, "Self-heating of cryogenic high electron-mobility transistor amplifiers and the limits of microwave noise performance", *Journal of Applied Physics*, vol. 132, no. 8, pp. 084501, 2022, doi:10.1063/5.0103156.

[25] Y. Zeng, "Low-Power HEMT LNAs for Quantum Computing", *Licentiate thesis, Department of Microtechnology and Nanoscience, Chalmers University of Technology*, 2023, https://research.chalmers.se/en/publication/537233.

[26] R. Reuter, M. Agethen, U. Auer, S. van Waasen, D. Peters, W. Brockerhoff, F.J. Tegude, "Investigation and modeling of impact ionization with regard to the RF and noise behavior of HFET", *IEEE Transactions on Microwave Theory and Techniques*, vol. 45, no. 6, pp. 977-983, 1997, doi:10.1109/22.588612.

[27] D. C. Ruiz, T. Saranovac, D. Han, O. Ostinelli, C.R. Bolognesi, "Impact ionization control in 50 nm low-noise high-speed InP HEMTs with InAs channel insets", *2019 IEEE International Electron Devices Meeting (IEDM)*, 2019, doi:10.1109/IEDM19573.2019.8993654.

[28] H. L. Hartnagel, R. Katilius, A. Matulionis, "Microwave noise in semiconductor devices", *John Wiley & Sons*, 2001.

[29] I. Esho, A. Y. Choi, A. J. Minnich, "Theory of drain noise in high electron mobility transistors based on real-space transfer", *Journal of Applied Physics*, Vol. 131, no. 8, 2022, doi:10.1063/5.0069352.

[30] C-H Chen, M.J. Deen, "Channel noise modeling of deep submicron MOSFETs", *IEEE Transactions on Electron Devices*, vol. 49, no. 8, pp. 1484-1487, 2002, doi:10.1109/TED.2002.801229.